Investigation of the Swelling Response and Loading of Ionic Microgels with Drugs and Proteins: The Dependence on Cross-Link Density

Gary M. Eichenbaum,[†] Patrick F. Kiser,[†,‡] Andrey V. Dobrynin,[§] Sidney A. Simon,[⊥] and David Needham*[,†]

Department of Mechanical Engineering and Materials Science, Duke University, Durham, North Carolina 27708-0300; Access Pharmaceuticals, Dallas, Texas 75207-2107; Department of Chemistry, University of North Carolina, Chapel Hill, North Carolina 27599-3290; and Department of Neurobiology, Duke University Medical Center, Durham, North Carolina 27710

Received December 17, 1998; Revised Manuscript Received April 20, 1999

ABSTRACT: The pH and NaCl induced swelling response and drug and protein loading of poly(methacrylic acid-*co*-acrylic acid) microgels (4−10 μm diameter) were measured as a function of cross-link density. The swelling ratio (Q) of the microgels increased linearly from 2 to 12 when the mole fraction of cross-linking monomer decreased from 0.25 to 0.10 (at pH's > 5.3). In the presence of 5 M NaCl (at pH's > 5.3), microgels with cross-linking feed ratios of 0.25 and 0.10 swelled to only 80% and 60% of their maximum volume measured at low ionic strength, respectively. To determine the average pore size in the different cross-linking density microgels (feed ratios = 0.25, 0.20, 0.15, and 0.10), we measured the size cutoffs for the uptake of different sized proteins. On the basis of these size exclusion experiments, we calculated the number of monomers between cross-links in each of these gels to be 6.5, 9.5, 12.5, and 16.5, respectively. These values were used in our theoretical modeling of the network swelling (modified Flory−Huggins thermodynamic model) to predict the pH−Q dependence for different degrees of cross-linking. The model predictions of the microgel pH swelling response as a function of cross-link density were in good quantitative agreement with experiments. Experimentally, the loading of smaller drug molecules did not have clear molecular weight dependence for the different cross-link density microgels. However, differences in the loading behavior of these molecules on the basis of their partition coefficients indicated that binding affinity, molecular packing, and condensation were important factors that need to be explored to optimize microgels for use in specific drug delivery applications.

Introduction

The term "microgel" refers to a micrometer-in-diameter, spherical, covalently cross-linked polymer network. Ionic microgels contain fixed ionic groups bound to their backbone that give them ion-exchange properties. To date, few studies have focused exclusively on ionic gels at the micron size scale (i.e., 1−10 μm in diameter),[1,2] although there have been a number of studies on centimeter size "slab gels".[3−5] Microgels are characterized by their small size (∼1−10 μm) and faster response times than slab gels, 0.5 s versus hours to days, to reach swelling equilibrium when their ionic chemical surroundings are changed.[2]

As a result of these features, microgels are being explored for use in a number of new drug delivery and therapeutic applications.[6−11] Gels that are on the size scale of microns can travel in the bloodstream, and those that are on the size scale of fractions of a micron have the potential to be targeted to certain diseased tissues outside the bloodstream and even be taken up into the intracellular compartment of target cells.[12]

For use in these applications, it is critical to understand how microgel structure and composition determine their properties and performance is crucial. For example, the use of microgels in a drug delivery application requires an understanding of the effect that the network pore size has on the controlled molecular exchange of a drug or protein.[5,13,14]

Building upon previous studies on the effect of cross-linking density on the swelling response[4,13−16] and drug[5,13,17−21] and protein loading[20,22] of slab gels, in this paper we study for the first time the effect of cross-link density on the swelling and drug/protein loading in microgels. The work presented in this paper follows a previous study of individual 4−7 μm diameter poly(methacrylic acid) microgels, in which the swelling response was investigated for microgels with a single cross-link density.[2]

In this work, first we measured the effect of cross-link density on the microgel pH and NaCl swelling response. Next, using a new technique that employed protein loading, we measured the upper and lower bounds of the microgel pore size versus cross-link density. To further characterize the loading of the microgels for potential applications in drug delivery, we then studied the loading properties of two local anesthetics, benzylamine and dibucaine, and a chemotherapy drug, doxorubicin,[11] as a function of cross-link density. Finally, we used the experimentally measured pore sizes of the microgels as an input to a modified thermodynamic Flory−Huggins model to predict the pH−Q response of the microgels as a function of their degree of cross-linking. The experimental and model results for the swelling response and the experimental results for the drug and protein loading elucidate several important factors that need to be explored to design and optimize this system for specific drug delivery and therapeutic applications.

Materials and Methods

Poly(methacrylic acid) Microgel Synthesis. All of the microgels were synthesized by modifying the method developed

* To whom correspondence should be addressed.
[†] Duke University.
[‡] Access Pharmaceuticals.
[§] University of North Carolina.
[⊥] Duke University Medical Center.

10.1021/ma981945s CCC: $18.00
Published on Web 07/03/1999

Table 1. Starting Materials That Were Used in the Synthesis of the Four Different Cross-Linking Density Microgels

composition	cross-linker MBAM	MAC	NPA	solvents (vol %)
1	0.10	0.450	0.450	100% EtOH
2	0.15	0.425	0.425	100% EtOH
3	0.20	0.400	0.400	100% EtOH
4	0.25	0.375	0.375	75% MeOH, 25% EtOH

by Kawaguchi.[23,24] The same starting materials were used to synthesize microgels with four different degrees of cross-linking. All four compositions consisted of 4-nitrophenyl acrylate monomer (NPA), methacrylic acid monomer (MAA), methylenebis(acrylamide) cross-linker (MBAM), and azobis(isobutyronitrile) (AIBN). Table 1 shows the mole fractions of starting materials and solvents that were used in the synthesis of the different feed ratio (FR) microgels.

MBAM (Aldrich) was recrystallized twice from methanol at 50 °C; NPA was recrystallized from methanol and cooled to −60 °C before collecting the crystals. AIBN (Aldrich) was recrystallized twice from chloroform. MAA (Aldrich) was twice distilled at 30 °C under vacuum. All monomers and initiators were stored under argon at −20 °C. The monomers and initiator with the FR's listed in Table 1 were dissolved in the corresponding mixtures of alcohol solvents. We found that a less polar solvent was required to synthesize the 0.25 FR microgels. Because nitrophenol acts as a chain transfer agent, an excess molar mass of initiator to the amount of NPA monomer was required.[24] The reactions were degassed at room temperature for 20 min by bubbling argon into the alcohol solution. The flask containing argon was immersed in a mineral oil bath, and the reaction media was warmed to 60 °C**,** whereupon solid AIBN was added to the reaction. Within 3 min after the addition of the initiator, the solution became a cloudy dispersion of particles. The reactions were left unstirred, as stirring reduced the particle size. The reaction was run for 3 h. It was left standing until it reached room temperature. The sample was pelleted by centrifugation (2000 RCF) and then was resuspended in fresh ethanol. This process was repeated five times, and then the sample was dried to a constant weight (100 °C, 0.1 Torr for 12 h). The dried reaction product was subsequently suspended and then resuspended (four times) in 50 mL of 1 M NaOH (to hydrolyze the nitrophenol groups from the microgels and thus give a random copolymer between acrylic acid, methacrylic acid, and MBAM). To remove the hydrolysis products, the resulting microgel suspension was centrifuged and washed in distilled water four times. Finally, the beads were stored in deionized water at 4 °C.

Note we assume that the FR that was set during the synthesis was proportional to but not exactly equal to the cross-link density in the microgels. Thus, where exact numerical values were required, the FR was used. However, in qualitative descriptions throughout the paper the terms are used interchangeably.

Bulk Titration. We performed a bulk titration under an argon atmosphere to determine the apparent pK_a for each of the different cross-link density microgels. A stock solution of 100 mM HCl was injected into a suspension of microgels (45 mg in 45 mL) with 10 mM NaOH that was added to fix the initial sodium ion concentration at 6 mM and the pH of the titration at 11.4. A back-titration was then performed with 100 mM NaOH. Titrations with 100 mM HCl were repeated twice for each microgel composition at sodium concentrations of 0.006 and 0.014 M. Titrations of NaCl solution in the absence of microgels were performed at these same sodium concentrations and were subtracted from the microgel titrations. The methods and model that were used to determine the apparent pK_a and the capacity of the microgels were described previously.[2]

Micromanipulation of Microgels. The micropipet flow technique, which is centered on an inverted microscope, is a useful method for manipulating and observing the swelling response of individual microgels that have a diameter greater than 1 μm^2. This technique was used to measure the volume response of the microgels to changes in pH and ionic solution conditions. In a flow pipet experiment, an individual microgel was held by a holding pipet in a chamber, which contained a control solution. Positive pressures (500−1500 N/m^2) were applied to the "flow pipet" (∼20 μm i.d.), which was filled with a test solution, by using a 1 mL syringe acting onto the air gap of a second manometer reservoir. When this flow pipet was aligned axially with the microgel, the microgel became immersed in the flow field of the test solution. We repeated all of the micropipet manipulation measurements on all four different microgels. Note that, by using this technique to measure the swelling response of single microgels, the errors associated with diameter measurements of a bulk sample of microgels, as a result of microgel polydispersity, were significantly reduced.[2]

Solutions Used in the Measurements of the Volume Response. Buffered sodium citrate and phosphate buffer solutions were used in all of the measurements of the equilibrium swelling response (Q) of individual microgels, unless otherwise indicated. For the combined pH and NaCl concentration experiments, the citrate buffer solutions contained 10 mM citrate and ranged from pH 2.5 to 6.6 in approximately 0.2 pH unit increments. The phosphate buffer solutions contained 10 mM phosphate and ranged from pH 6.2 to 7.8. There were no differences between the microgel volumes in 10 mM phosphate and 10 mM citrate buffer at the same pH. For measurements of Q of the microgels in response to changes in NaCl concentration, the solutions contained 0.1 mM phosphate buffers with 0.001, 0.01, 0.1, 1.0, and 5.0 M NaCl, all at pH 7.8.

Macromolecule Loading. *Protein Uptake.* To obtain an estimate for the mesh size in the four different cross-link density microgels, a new method based upon protein loading was used. Five different sized globular proteins (dimensions ranging from 3.0 to 7.5 nm) with isoelectric points above pH 6.5, and thus positively charged, were incubated with the microgels. The net positive charges of these proteins at pH's above 6.0 ensured that they would load into the negatively charged gels by ion exchange.[11] Their uptake was monitored spectrophotometrically by measuring the absorbance versus wavelength (Shimadzu UV-1601).

Exclusion of the different sized molecules from a given cross-link density microgel was indicative of an upper bound on the matrix mesh size. The five proteins were trypsinogen from bovine pancreas (25 kDa), myoglobin from horse skeletal muscle (17.5 kDa), avidin from egg white (62 kDa), glyceraldehyde-3-phosphate dehydrogenase (GAPDH) from chicken muscle (140 kDa), and bovine catalase (232 kDa) (all were obtained from Sigma Chemical Co., St. Louis, MO). Protein structures were downloaded from the protein databank (NIH). The linear dimensions of the crystal structures of each of the proteins were estimated using RasMol.[25] The crystal structures provided us with a reasonable first-order approximation of the space occupied by the proteins in the microgel. The fact that a bulk volume condensation of the microgels was observed when the proteins loaded suggested that the proteins and microgel were dehydrated from their hydrated states in solution.

To prevent any loss of protein due to adsorption of protein on the tubes and pipet tips, all surfaces that would be exposed to protein solutions were incubated in 1 mg/mL bovine serum albumin (Sigma) prior to any of the protein uptake experiments. All of the protein solutions were prepared in deionized water at concentrations of 1 mg/mL. The four different microgel compositions were each dried to constant weight (in three separate vials) and were resuspended in deionized water at a concentration of 1 mg/mL. A 50 μL aliquot of each of the four cross-link density microgels was then added to 450 μL of each protein solution. To ensure that the proteins would load by ion exchange for the sodium counterions in the microgels, the pH of each suspension was adjusted to a range between 6.10 and 7.00, bracketed by the pK_a of the microgels and the pI's of each protein. The pH was adjusted by the addition of submicroliter quantities of 0.5 M NaOH and 0.5 M HCl. As a result of the limits on the pH ranges in which we could

measure the uptake of each protein, it was not possible to standardize the total charge on the proteins during loading. The pH of each suspension was as follows: trypsinogen (pH 6.5), myoglobin (pH 6.75), avidin (pH 7.0), GAPDH (pH 7.0), and catalase (pH 6.1).

The resulting suspensions of microgels and proteins were then placed on an orbitron rotator II (model 260250, Boekel Industries, Inc.), until the system had reached steady-state equilibrium (in the sense that no change in absorbance of the supernatant was observed after 4−5 h). Any shifts in pH after incubation were adjusted to the original pH's listed above by the addition of submicroliter quantities 0.5 M NaOH and 0.5 M HCl. Finally, the suspensions were pelleted by centrifugation (RCF 3000) for 15 min (Marathon Micro A, Fisher Scientific).

Measurements of absorbance versus wavelength were made on the supernatant solutions of the protein/microgel suspensions and a control solution that contained protein but had never been exposed to the microgels. Appropriate dilutions were made to obtain absorbance readings in the linear range of Beer's law. Absorbance readings for trypsinogen, myoglobin, avidin, GAPDH, and catalase were made at 195.5, 407.5, 192.5, 190.5, and 192.5 nm, respectively. The entire procedure was performed in triplicate for each protein and different cross-link density microgel. The uptake of protein by the microgels (milligram of protein per milligram of microgel) was calculated using eq 1

$$\text{uptake}\left(\frac{\text{mg of protein}}{\text{mg of microgel}}\right) = \frac{A_c - A_r}{A_c} V_{sys} m_{gel}^{-1} C_{stock} \quad (1)$$

where A_c and A_r are the absorbance of the control and reaction supernatant solution, respectively, V_{sys} is the volume of system, m_{gel} is the mass of microgels in the system, and C_{stock} is the concentration at which the protein stock solution was prepared.

Small Ionic Molecule/Drug Uptake. To measure the bulk loading of cationic anesthetics and an anticancer drug into the different cross-link density microgels, we chose three monovalent, cationic molecules that have increasing molecular weight and complexity. They were benzylamine hydrochloride (MW 143.6 g/mol), dibucaine hydrochloride (MW 379.9 g/mol), and doxorubicin hydrochloride (MW 580.0 g/mol) (obtained from Sigma Chemical Co, St. Louis, MO).

The loading experiments and absorbance measurements were carried out in the same way as described above for the protein loading experiments and were repeated three times for each small molecule/microgel combination. The maximum wavelengths for the absorbance measurements of benzylamine, dibucaine, and doxorubicin were 206.0, 208.0, and 481.5 nm, respectively. A 50 μL aliquot of each of the different cross-link density microgels (prepared at 1 mg/mL in deionized water) was combined in separate vessels with 450 μL aliquots of 3.00 mM benzylamine in deionized water, 3.00 mM doxorubicin in 10 mM tris buffer, and 1.50 mM dibucaine in deionized water. The concentration of each cationic molecule was set at a sufficient level to achieve the maximum loading. The maximum loading level was determined by removing the supernatant solution, resuspending the microgels in fresh stock solution, and then measuring for additional uptake. In a similar manner as for the protein loading experiments, the pH of each suspension was adjusted to a range between 6.25 and 7.0, a range that was between the pK_a of the microgels and the pK_a of each molecule. Experiments were run at pH 6.25 for dibucaine and pH 6.75 for benzylamine and doxorubicin.[26−28]

To measure the volume change of the microgels when they were loaded with the local anesthetics and doxorubicin, we used the micropipet flow technique described above. Individual microgels were immersed in test solutions that contained the drug, and their volume change was measured by video microscopy.[2]

Experimental Results and Discussion

Effect of Changes in Solution pH on Microgel Volume. Video images of the lowest feed ratio (FR = 0.10) and highest feed ratio (FR = 0.25) microgels in pH 7.8 and 2.0 buffer are shown in Figure 1. It is evident that the gels are more expanded at the higher pH (Figure 1, A1 and B1) and that the lowest FR microgel swells to a much larger volume than the highest FR microgel. The condensation of the microgels in pH 2.0 buffer arises from the exchange of protons for sodium ions and a subsequent reduction in the osmotic swelling pressure inside the microgel.[29] Figure 2 shows a plot of the equilibrium swelling ratio, Q (Q = the ratio of the volume of a microgel at the test pH to its volume in its most condensed state), versus pH for microgels that were suspended in a citrate buffer solution at the pH indicated. For a FR of 0.10, increasing the pH from 1.7 to 7.8, while holding the buffer ion concentration constant, produced an increase in Q from 1 to 12.7. Note that for pH's < 3.6 all the different feed ratio microgels reached their minimum volume, and for pH's > 5.3 they were in their most expanded state. These results were consistent with the dependence of swelling on cross-link density that has been observed for slab gels.[4,13,16,30]

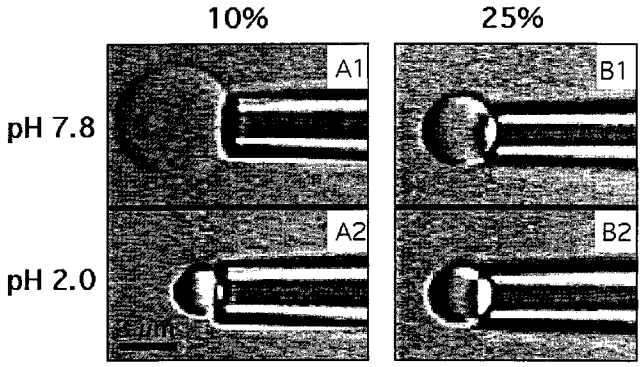

Figure 1. Video images of poly(methacrylic acid-*co*-acrylic acid) microgels held by micropipets and suspended in different pH citrate buffer solutions. (A1) Most expanded state: 0.10 FR microgel in pH 7.8 buffer. (A2) Most condensed state: the same 0.10 FR microgel as A1 in a pH 2.0 buffer. (B1) Most expanded state: 0.25 FR microgel in pH 7.8 buffer. (B2) Most condensed state: the same 0.25 FR microgel as B1 in a pH 2.0 buffer.

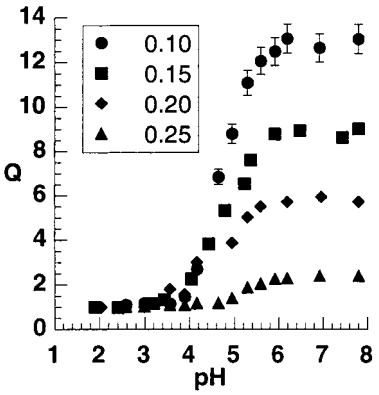

Figure 2. Plot of the equilibrium swelling ratio (Q) for the different cross-link density microgels versus the pH of the external solution. Error bars on each data point represent the standard deviation of the average swelling ratio of five different PMAA microgels.

Figure 3 shows that the maximum swelling (Q_{max}) at pH's > 5.3 decreased linearly with the FR (0.10−0.25), which is proportional to the degree of cross-linking. Thus, the greater the extent of cross-linking, the less the gels swelled from their most condensed state when placed in the high-pH solutions.

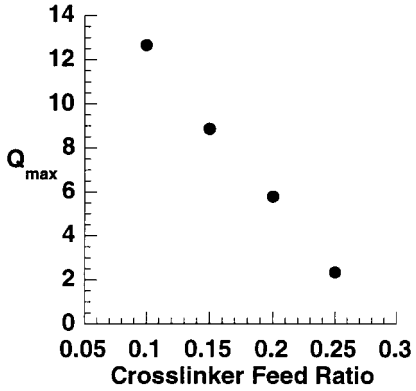

Figure 3. Plot of the maximum swelling (Q_{max}) for the different cross-link density microgels versus the feed ratio for the pHs greater than 5.3. Each data point represents the average volume ratio of five different microgels at the indicated degree of cross-linking. The largest Q was observed for a microgel with a FR of 0.10.

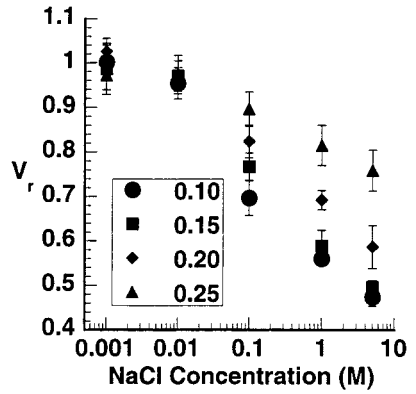

Figure 4. Plot of V_r for the different cross-link density microgels versus NaCl concentration in the high pH regime (pH > 5.3). Each data point represents the average volume ratio of five different microgels at the indicated NaCl concentration. The largest NaCl induced V_r of 0.62 was observed in 5 M NaCl.

Effect of Changes in NaCl Concentration on Microgel Volume. Figure 4 shows a graph of V_r (= $1/Q$), the ratio of the microgel's volume at pH > 5.3 to their maximally swollen volume against NaCl concentration. The extent by which V_r was reduced increased with NaCl concentration and decreased with the FR. For all of the different FR's, V_r decreased linearly with increasing NaCl concentration. For the microgels with a FR of 0.25 in 5 M NaCl, V_r was 0.75. In contrast, for the lower cross-linking density gels (FR's = 0.20, 0.15, and 0.10), V_r was 0.53, 0.48, and 0.45, respectively.

For all FR values, V_r in the presence of NaCl was less than in the presence of protons (0.45 for NaCl versus 0.10 for protons). A primary reason for this difference was that the sodium counterions do not bind to carboxyl groups as strongly or as tightly as protons do. As a result, they have more water associated with them and thereby generate a larger osmotic swelling pressure opposing condensation.[31] For more details, see Eichenbaum et al.[2]

Effect of Cross-Linking Density on Molecular Loading. There were two goals of the loading experiments: (1) to measure the pore size in the different cross-link density gels by protein size exclusion and (2) to quantitate the loading of two local anesthetics, benzylamine and dibucaine, and a chemotherapy drug, doxorubicin, as a function of the cross-link density. It was not meaningful to quantitatively compare the degree of loading of the proteins and the drugs because we could not standardize the net positive charge on the proteins (see Methods section).

Protein Loading/Exclusion. To measure the average pore size of the different cross-link density microgels at pH's > 6.0, four positively charged globular proteins were incubated with the microgels. The shortest cross-sectional dimensions of these proteins ranged from 3.5 to 7.5 nm (obtained from crystallography) with the microgels. Under these conditions, there was an electrochemical potential gradient driving the proteins to exchange with sodium ions and load into the anionic microgels. In cases where the average pore size in the gel was smaller than the effective diameter of a protein, that protein was sterically excluded from the microgel matrix (measured by UV absorbance of the supernatant solution). Thus, to obtain an estimate for their range of pore sizes, we determined whether a protein loaded or was excluded from each cross-link density microgel.

To determine whether the spectraphotometric loading measurements were indicative of a bulk or surface loading, micropipet manipulation experiments were conducted. We observed that the microgels underwent a bulk condensation when they were immersed in the solutions of the proteins that were not excluded (as measured spectrophotometrically). This observation suggested that there was a bulk loading of the proteins into the microgels.

Figure 5 shows the spectra of the absorbance versus wavelength for all of the protein loading experiments into the four different FR microgels and the control, which consisted of protein solution at the same dilution factor as the microgel suspensions but that had not been exposed to any microgels. Focusing on the case of avidin, for FR's of 0.20 and 0.25, there was not a significant difference in the intensities of the absorbance spectra between the solutions containing the microgels and the avidin control, indicating that the protein did not load into these microgels. However, in the cases of the 0.10 and 0.15 FR gels, there was a significant decrease in the intensities of the absorbance spectra, indicating that avidin was removed from the suspending solution and had loaded into these microgels.

Figure 6 shows a graph of the loading of four different proteins into all four FR microgels. It is evident from the plot that all of the proteins shown in the plot loaded into the gels with a FR of 0.10, although less GAPDH loaded into these gels than the other FR gels. The total exclusion of bovine catalase (not shown in Figure 6 because it was completely excluded from all FR's, see Figure 5) and partial exclusion of GAPDH from the 0.10 FR microgels (statistically significantly different than the other proteins taken up for this FR, t-test, $\alpha = 0.05$) indicated that their average pore size lies between 6.5 and 8.5 nm, the range of the minimum end-to-end distance for bovine catalase and GAPDH. For the gels with a FR of 0.15, the partial loading of avidin and exclusion of GAPDH indicated that the average pore size was between the 5.5 nm minimum end-to-end distance for avidin and the 6.5−7.5 nm minimum end-to-end distance for GAPDH. In the case of the gels with a FR of 0.20, GAPDH and avidin were excluded from the microgels, whereas myoglobin and trypsinogen were loaded. This indicated that the average pore size for the 0.20 FR gels was between the 4.4 nm minimum end-to-end distance for myoglobin and the 5.5 nm minimum

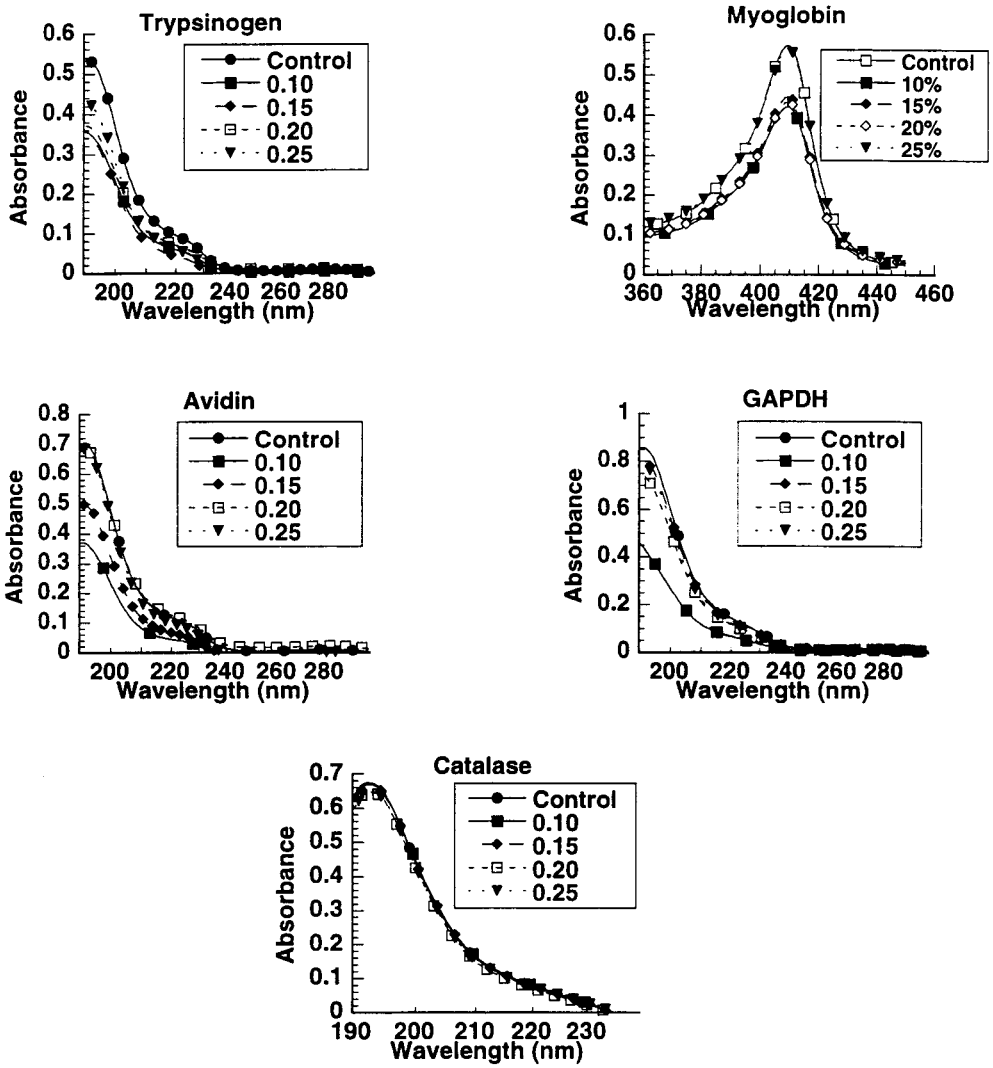

Figure 5. Spectra plotted as absorbance versus wavelength for the protein loading of the four different FR microgels. The control spectrum was for the loading solution in the absence of microgels. Note that avidin was excluded from the 0.20 and 0.25 FR microgels.

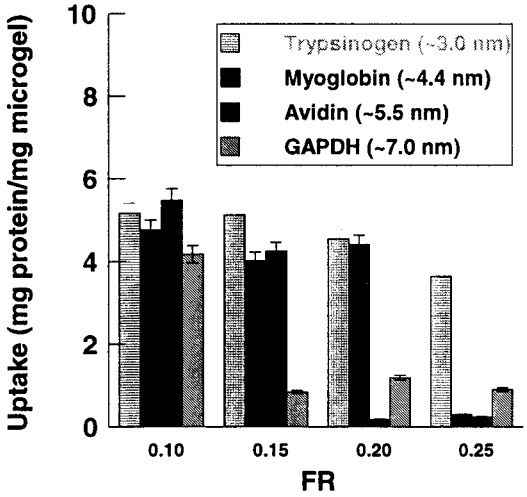

Figure 6. Plot of the trypsinogen (MW = 25 kDa, dimension = 3.0 nm), myoglobin (MW = 34 kDa, dimension = 4.4 nm), avidin (MW = 62 kDa, dimension = 5.5 nm), and GAPDH (MW = 140 kDa, dimension = 7.5 nm) loading into microgels of FR 0.10, 0.15, 0.20, and 0.25.

end-to-end distance for avidin. Finally, in the case of the gels with a FR of 0.25, with the exception of trypsinogen, all of the proteins were excluded from the microgels. This indicated that the average pore size was between the 3.0 nm minimum end-to-end distance of trypsinogen and the 4.0 nm minimum end-to-end distance of myoglobin.

The crystal structures of the proteins that were used in the loading experiments, as well as schematic representations of the pore dimensions of the different cross-link density microgels (all drawn to scale) that were deduced from the loading experiments, are shown in Figure 7. The fact that a bulk volume condensation of the microgels was observed when the proteins loaded suggested that the proteins and microgel were dehydrated from their hydrated states in solution and that the crystal structures provided a reasonable estimate for the pore size.

Drug Loading. Figure 8 shows the molecular structures of the three cationic drugs that were loaded into the microgels.[27,28,32] These compounds were chosen because of their potential therapeutic value, similarity in being monovalent cationic weak bases, and increasing size, water solubility, and chemical complexity. Like the proteins investigated, the net positive charges of these drugs at pH's above 6.0 provided a driving force for them to load into the negatively charged gels by ion exchange.[11] A summary of the properties of the drugs is shown in Table 2.

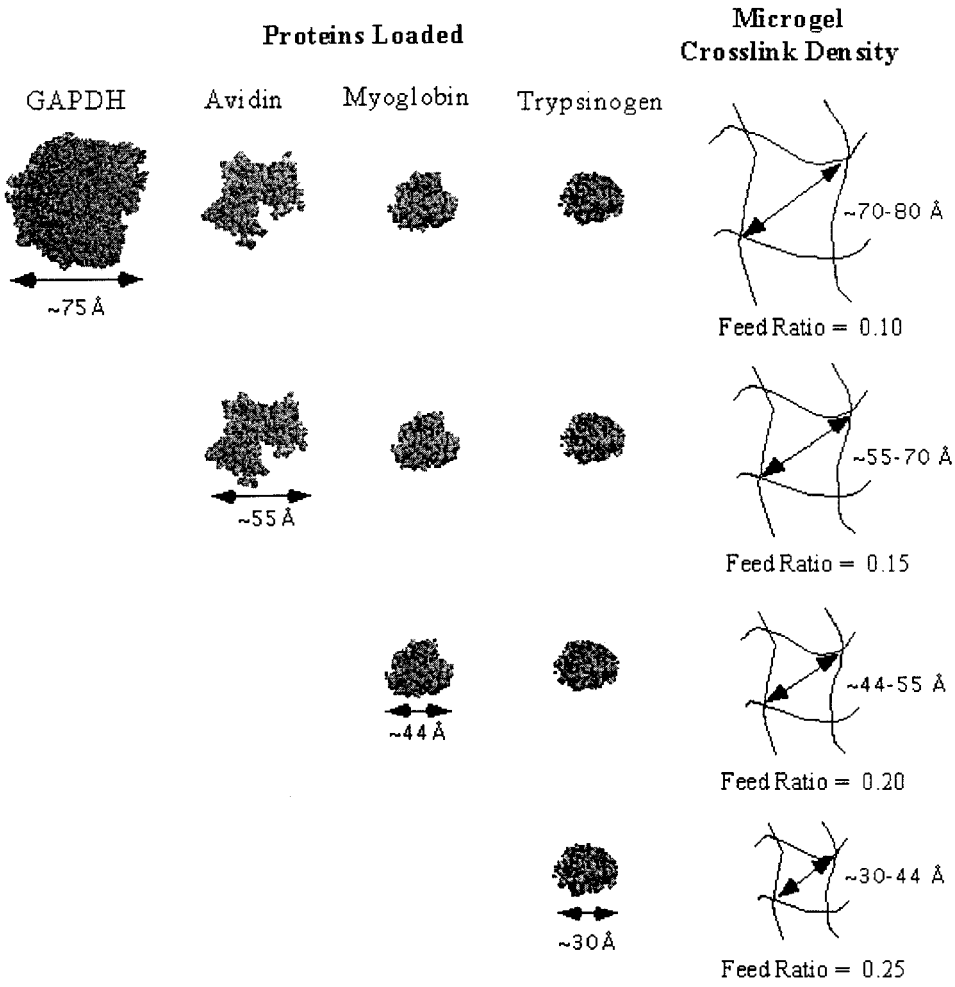

Figure 7. Schematic diagram showing the estimated range of pore sizes in the different cross-link density microgels based upon the protein loading experiments (see text).

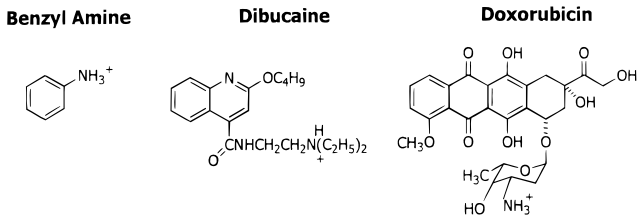

Figure 8. Molecular structures for the compounds that were used in the small molecule loading studies.

Figure 9 shows a plot of the loading of protons (as measured by bulk titration), benzylamine, dibucaine, and doxorubicin for the four different FR microgels. It is evident from the plot that the capacity of all of the microgels for protons exceeded their capacity for any of the larger cationic molecules. The loading of benzylamine was independent of the FR and lower than that of dibucaine or doxorubicin for the 0.10 and 0.15 FR gels. In contrast, the loading of dibucaine and doxorubicin decreased from 5.19 mequiv/g for the 0.10 FR gels to 3.54 mequiv/g for the 0.25 FR gels. It is unlikely that the sole reason for this difference is the larger size of the dibucaine, 379.9 g/mol, and doxorubicin, 580.0 g/mol, as compared to benzylamine, 143.6 g/mol.

To better understand the source of these differences in loading behavior, we used the micropipet flow technique to measure the volume changes of the four FR microgels when they were loaded with each of the cationic molecules (Figure 10). In Figure 10, it was

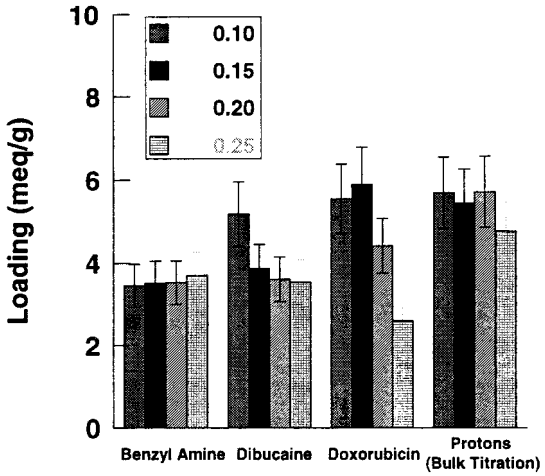

Figure 9. Plot of the amount of small macromolecule/drug loading as a function of the feed ratio. Note that proton loading was measured by bulk titrations of the microgels.

evident that the loading of dibucaine and doxorubicin caused a volume condensation and a change in the refractive index of the microgels that was distinctly different from their refractive index due to a pH induced condensation (Figure 1).

Figure 11 shows a plot of V_r of the four different FR microgels when they were loaded with the benzylamine, dibucaine, and doxorubicin. On average, when loaded with benzylamine, dibucaine, and doxorubicin the V_r's

Table 2. Parameters Describing the Drugs Used in the Loading Studies

drug/ molecule	MW (g/mol)	vol (Å^3)	octanol/water partition coeff (log *P*)
proton	1	N/A	N/A
benzylamine	143.6	27.6	1.07
dibucaine	379.9	135.5	2.52
doxorubicin	580.0	450.5	1.85

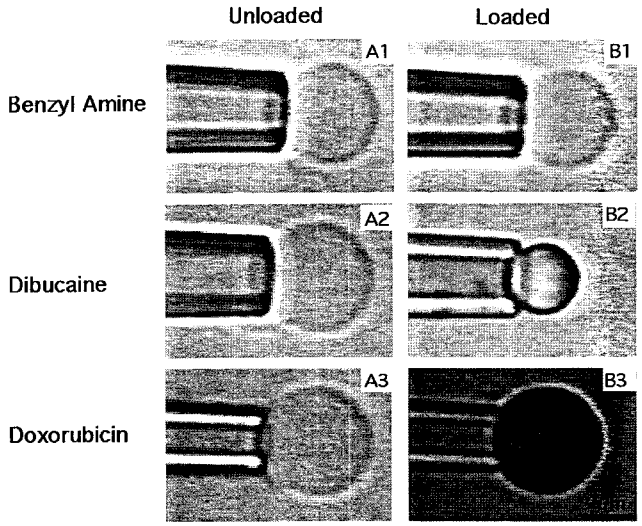

Figure 10. Panels A1, A2, and A3 show video micrographs of three different 0.10 FR microgels that were unloaded and fully swollen in pH 7.0 citrate buffer. Panels B1, B2, and B3 show the same three microgels that were loaded and condensed with benzylamine, dibucaine, and doxorubicin, respectively. The video micrographs of the benzylamine loaded gels were visually indistinguishable from the control of a microgel immersed in buffer with no drug present.

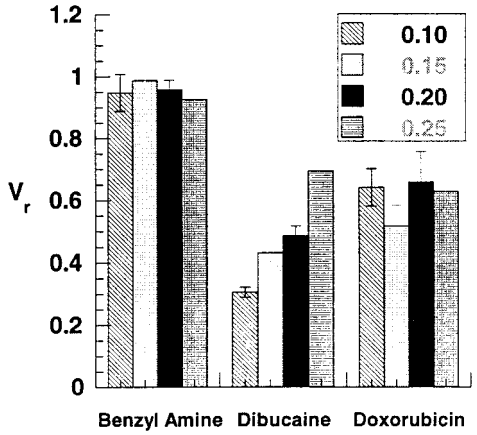

Figure 11. Plot of the fraction V_r for the four FR microgels loaded with benzylamine, dibucaine, and doxorubicin. The control, which consisted of a microgel immersed in a buffer solution with no drug present, had a V_r of 1.

were 0.9, 0.5, and 0.7, respectively. It was evident from the plot that benzylamine did not significantly condense any of the microgels when it loaded. This implied that the interaction and binding of benzylamine molecules in the microgels was comparable to that of the hydrated sodium counterions for which they exchanged. A weaker interaction between benzylamine and the ionic network was consistent with the lower degree of loading of benzylamine as compared to the cases of dibucaine and doxorubicin.

The magnitude of the volume reduction associated with the dibucaine loading was the largest of the three molecules, decreasing from a V_r of 0.30 to 0.70 for the 0.10 and 0.25 FR microgels, respectively. This decrease in the volume reduction between the 0.10 and 0.25 FR microgels was consistent with the 1.65 mequiv/g decrease in dibucaine loading between these FRs. It suggested that the volume available in the collapsed 0.25 FR microgels limited the loading of dibucaine.

For the doxorubicin loading, the different FR microgels all condensed to the same extent. This implied that at equal degrees of condensation there was a larger free volume available for doxorubicin loading into the two lower FR microgels as compared to the two higher FR microgels. This result was consistent with the higher loading (by 1.65 mequiv/g) of doxorubicin into the 0.10 and 0.15 FR microgels as compared to the 0.20 and 0.25 FR microgels.

These loading results suggest that the binding and subsequent dehydration and collapse of the microgel matrix play an important role in determining the degree of loading of the microgels. To understand the cause of the overall differences in the microgels' average V_r upon loading (V_r's were 0.9, 0.7, and 0.5 for benzylamine, doxorubicin, and dibucaine, respectively), we compared the drugs' octanol−water partition coefficients, *P*. The log *P*'s for benzylamine, doxorubicin, and dibucaine were 1.07, 1.85, and 2.52, respectively.[33] These partition coefficients indicated that it was more thermodynamically favorable for dibucaine (log $P = 2.52$) to reside in a less polar environment than benzylamine (log $P = 1.07$). Thus, dibucaine, which had the highest partition coefficient, dehydrated the microgels to the largest extent ($V_r = 0.5$), and benzylamine, which had the smallest partition coefficient, condensed the microgels the least ($V_r = 0.7$). Because the microgel matrix pore size changed when the matrix condensed, steric constraints as well as variations in the intermolecular interactions and packing of these different molecules within the matrix were expected to have played an important role.

Model Results and Discussion

Thermodynamic Model To Predict Equilibrium Swelling. To obtain a quantitative explanation for the swelling versus pH curves (Figure 3), we have modified existing Flory−Huggins thermodynamic theory for the swelling of ionic networks to predict the pH swelling response of the microgels as a function of their degree of cross-linking.[34,35] We chose this model because of its successful application to describe the pH swelling response of ionic slab gels.[3,4,14,35−39]

The primary modifications to the existing model included (1) the use of a term to account for counterion binding in the matrix, because of the high density of fixed charges in the microgels (3.0 M), (2) the inclusion of a term to account for the change in solubility of the microgels with pH/polymer volume fraction (this entailed using a variable Flory χ parameter), and (3) the use of a non-Gaussian expression for the elasticity to account for the high cross-linking density in the microgels (6.5 and 16.5 monomers between cross-links based upon an FR of 0.25 and 0.10, respectively). A complete derivation of the model can be found in Appendix B.

Model Inputs. The inputs that were used in the model are summarized in Table 4. For each of the microgel cross-link densities, we used the same value of ρ, the density of pure polymer in the microgels, as was measured experimentally.[2] The value for ϕ_o, the

Table 3. Values of the Constants in Eq B9 for Different Polymer/Water Systems

polymer	χ_o	b	ref
poly(methacrylic acid gels)	0.42	0.60	30
poly[*N*-(2-hydroxypropyl)-methacrylamide]	0.47	0.489	45
poly(2-hydroxyethyl methacrylate-*co*-methacrylic acid)	0.51	N/A	46
poly(vinyl alcohol)	0.46	0.456	47

Table 4. Values for the Inputs to the Thermodynamic Swelling Model

input	value		source
K_a	$10^{-4.7}$		measured
K_{Na}	0.25		ref 52
C_{Na} bulk	0.03 M		experiment
ρ polymer	0.85 cm^3/g		measured
ϕ_o	0.8		measured
V_1	18 cm^3/mol		CRC
χ	$0.45 + 0.489\phi$		ref 53
$C_{carboxyl}$	5.77 mequiv/g		measured
FR	N	M_{mer}	measured, adjustable parameter
0.25	6.5	86 g/mol	
0.20	9.5	90 g/mol	
0.15	12.5	94 g/mol	
0.10	16.5	97 g/mol	

ratio of the microgels' dry volume to their condensed volume, was measured by video microscopy and was the same within experimental measurement error (±0.02) for all of the FR microgels. The functional relationship that was used for χ is discussed in Appendix B. The number of carboxyl groups in a known mass of microgels was measured by bulk titration for each of the different cross-linking density microgels. The polymer volume fractions that were predicted by the model at each pH were referenced to the polymer volume fraction of the microgels in their most condensed state.

The values for N, the number of monomers between cross-links in the different gels, were deduced from experimental measurements on gel pore sizes (see Figure 7). Specifically N was calculated by solving for the number of mers of dimension 0.24 nm, connected to a single cross-linking mer with a dimension of 0.9 nm (one cross-linking monomer per pore) that would occupy a linear dimension equal to the experimentally measured pore sizes. These linear dimensions for the mer and cross-linker were estimated from an analysis of the known bond lengths and angles of their molecular structures in ChemDraw. The values of N were adjusted by using best-fit values within their experimentally measured range of corresponding pore sizes.

The mer average molecular weight, M_{mer}, of each of the four different cross-link density microgels was estimated using a weighted average of the molecular weights of the monomers between cross-links. This calculation took into account the number of mers between cross-links, N, and included the molecular weight of a single MBAM cross-linking monomer. Thus, M_{mer} increased from 86 g/mol for the FR = 0.10 microgels to 97 g/mol for the FR = 0.25 microgels.

Model Predictions of the pH Swelling Response and Comparison with Experiment. We will first describe the results of the model to predict the pH swelling curves for the different cross-link density microgels (Figure 3). The model predictions and experimental results are presented in Figure 12. The data show that there is quite good quantitative agreement between theory and experiment ($R^2 \geq 0.95$, t-test) over the entire pH range for all four microgel FR's. In addition, the model reveals the linear relationships between the experimentally measured adjustable parameter N, the FR of the microgels (Figure 13a), and the Q values at pH's > 5.5 (Figure 13b). The relationship between N and the cross-link density implies that there is a direct relationship between the molecular dimensions inside the microgel matrix and the feed ratio that was used in the synthesis.

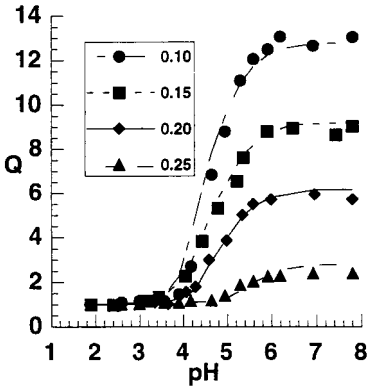

Figure 12. Plot showing a comparison of the experimental results and model predictions for the pH swelling response of the four different cross-link density microgels.

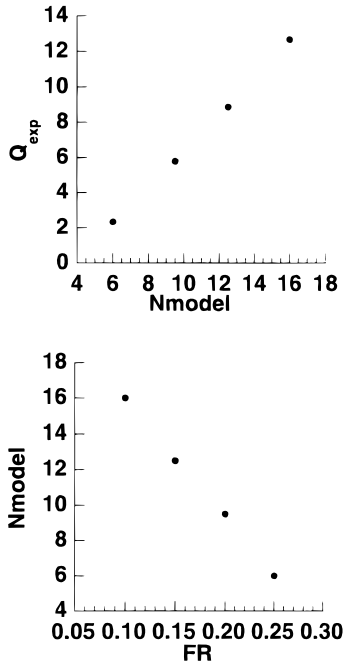

Figure 13. (a, top) Plot of N, the number of monomers between cross-links, versus the experimental swelling ratio at pH's greater than 5.5 for the four different cross-link density microgels. (b, bottom) Plot of the experimental feed ratio of cross-linking monomer versus N for the four different cross-link density microgels.

Model Predictions of the Microgel Modulus as a Function of pH. The theoretical model, described in the previous section, was used to estimate the bulk modulus of the microgels as a function of pH. In a regime below their elastic limit, polyelectrolyte gels swell to the concentration at which their bulk modulus, G, equals the osmotic pressure.[35,40,41] At low salt concentrations the osmotic pressure is dominated by counterions and is on the order of kT per free counterion. To confirm that the swelling response of the microgels that were studied experimentally was in the low-salt

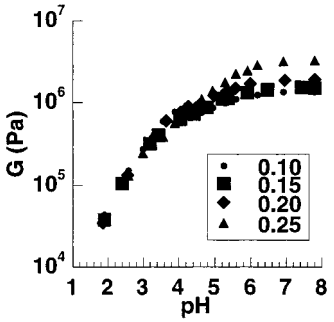

Figure 14. Theoretical plot using eq 2 of the modulus of the four different cross-link density microgels as a function of pH.

limit, we plotted the osmotic pressure at each corresponding pH versus concentration of counterions inside a microgel c/A, where $1/A$ is the fraction of dissociated charged groups on the polymer backbone. The value of the parameter A was calculated using the Donnan model described in Appendix B. The slope of 1 ($R^2 = 0.99$) for π vs c/A indicated that the microgels were indeed in the low-salt regime and that the osmotic pressure was kTc/A. This gives the estimate for the modulus of a microgel

$$G = \pi = \frac{c}{A}kT \tag{2}$$

Using eq 2, we obtained a plot of the bulk modulus ($G = \pi$) of the four different cross-link density microgels as a function of pH (Figure 14). The most important information contained in Figure 14 revealed that for all cross-link densities the modulus of the microgels increased about 2 orders of magnitude, from $\sim 10^4$ Pa at pH 2.0 to $\sim 10^6$ Pa at pH 7.8. The model also predicted that at pH's > 5.5, as the cross-linking density increased from 0.10 to 0.25, the modulus would increase from ~1 to ~3 MPa. We attribute this to the increased concentration of counterions per chain.

We have obtained qualitative evidence, using the micromanipulation technique, to support the predictions that the microgel bulk modulus increased when the pH was raised from 2.0 to 7.8. In Figure 15, we show a sequence of images of a microgel, suspended in pH 2.0 buffer, before, during, and after a force was applied to it by a glass bead. In response to the application of the mechanical force by the glass bead, a mechanical deformation of the microgel was clearly observed. In contrast, when the same force was applied to the same microgel, suspended in pH 7.8 buffer, no mechanical deformation was visible.

The model predictions for the bulk moduli of the microgels were in agreement with the qualitative experimental measurements that have been made on anionic slab gels of similar composition to the microgels[30,42] and naturally occurring micron scale polyelectrolyte gels.[43] For poly(acrylic acid) slab gels, Schossler et al. have observed an increase in the modulus from $\sim 10^5$ Pa at low pH to $\sim 10^6$ Pa at high pH. For poly(methacrylic acid) slab gels. Hasa et al. have observed an increase in the modulus from $\sim 10^4$ Pa at low pH to $\sim 10^5$ Pa at high pH.

Conclusion

In this paper we examined the effect of the degree of cross-linking on the pH and NaCl swelling response and the molecular and macromolecular loading of ionic microgels. We found that the swelling ratio of the microgels increased linearly from 2 to 12 when the mole fraction of cross-linking monomer decreased from 0.25 to 0.10 (at pH's > 5.3). We used Flory−Huggins theory, modified to account for ion binding, the change in the Flory interaction parameter with swelling, and the non-Gaussian elasticity of the microgel matrix, to quantitatively predict the equilibrium swelling of the microgels as a function of pH. The model also provided us with an estimate for the pH dependence of the microgel modulus that was in agreement with the experimental results.

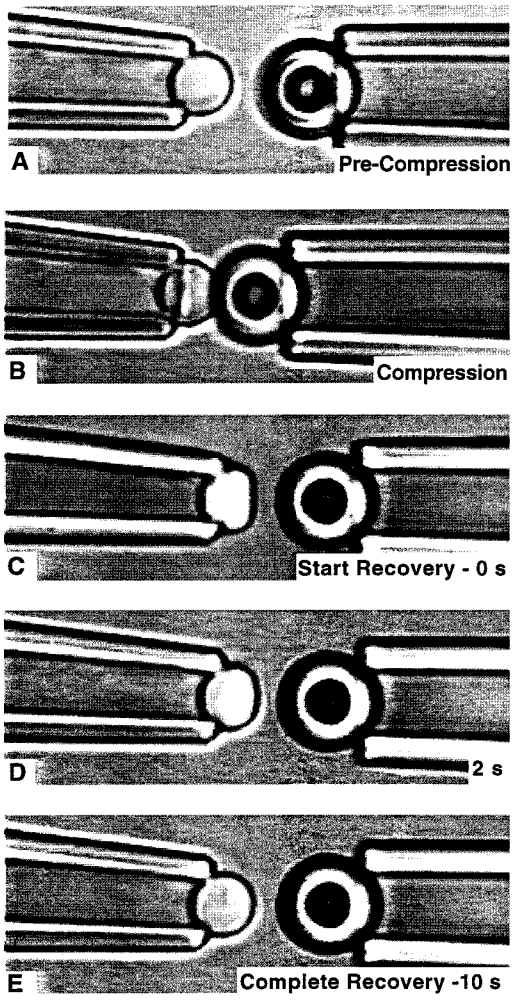

Figure 15. Video micrograph sequence of the compression of a microgel (left pipet) by a glass bead (right pipet) in pH 2.0 buffer. The sequence was as follows: (A) precompression, (B) compression, (C) retraction of glass bead, microgel showed deformation (time = 0 s), (D) partial recovery (time = 2 s), and (E) full recovery (time = 10 s).

Through a series of protein loading and exclusion experiments, we determined the range of pore sizes in the microgels, as a function of their degree of cross-linking. We showed that the microgels load high concentrations of protein in a cross-link density dependent manner. These results have important implications for the design and application of these microgels to protein delivery. We observed that drug and small molecule loading into the different cross-link density gels did not have clear molecular weight dependence and that there were small differences in the loading behavior for the different molecules studied. Consistent with the conclusions of Kim et al.[5] for the drug loading of slab gels, these results suggest that binding affinity, microgel condensation upon loading, and drug packing appeared

to be important factors that need to be explored to optimize microgels for use in specific drug delivery applications.

Acknowledgment. We thank Professors George Pearsall, Michael Rubinstein, and Doncho Zhelev for helpful discussions. We gratefully acknowledge financial support from Access Pharmaceuticals and the Duke University Center for Cell and Biosurface Engineering NIH Training Fellowship, North Carolina Space Grant Consortium, NIH-GM 27278 and NIH-GM 40162.

Appendix A. Nomenclature

A	number of monomers between uncondensed charges
A_c	absorbance of the control solution
A_r	absorbance of the supernatant in the reaction solutions
b	the slope for the functional dependence of the χ parameter on ϕ
c	monomer concentration (number density)
c_s	salt concentration (number density of each monovalent salt ion)
E	modulus of the gel
F_{el}	elastic part of the free energy of a gel
F_{mix}	mixing part of the free energy of a gel
F_{os}	osmotic part of the free energy of a gel
FR	feed ratio of cross-linking monomer in the microgels
G	bulk modulus
k	Boltzmann's constant
mer	average monomer repeat unit of the polymer chain
M_c	monomer average molecular weight
N	number of monomers in a gel strand
P	octanol−water partition coefficient
Q	equilibrium swelling (ratio of a fully swollen gel volume to its condensed volume)
Q_{max}	maximum equilibrium swelling ratio in pH 7.8 buffer, 0.01 M NaCl
T	temperature
V_r	ratio of the microgel volume in the presence of a given pH, NaCl and or drug concentration fully swollen microgel volume in pH 7.8 buffer, 0.001 M NaCl
χ	Flory interaction parameter
χ_o	Flory interaction parameter at infinite dilution
ϕ	volume fraction of polymer
λ	Donnan ratio
μ_{el}	elastic part of the chemical potential of a gel
μ_{mix}	mixing part of the chemical potential of a gel
μ_{osm}	osmotic part of the chemical potential of a gel
π	osmotic pressure of a semidilute solution at the same concentration as the gel
ρ	density of polymer

Appendix B. Model Derivation

At a fixed pH and NaCl concentration, the extent that a hydrogel swells is set by an energy balance between the osmotic pressure in the polymer matrix and the elastic energy of the network.[36] In uncharged gels the osmotic pressure arises from the configurational entropy of the chains (kT per chain). In polyelectrolyte gels the polymer contribution to the osmotic pressure is often dominated by the osmotic pressure arising from the concentration of fixed ionic groups in the gel and in turn to the reduction of the translational entropy of free ions associated with these ionic groups.[13,41,44] The elastic energy of the microgel network is controlled by the degree of cross-linking in the polymer matrix and is set during the synthesis of the gel.

Following the usual affine assumption, we split the total free energy of the system, F_{total}, into an osmotic, elastic, and a mixing free energy, F_{os}, F_{el}, and F_{mix}, respectively (eq B1).[35]

$$F_{total} = F_{os} + F_{el} + F_{mix} \tag{B1}$$

Taking the derivative of each of the terms in eq B1 with respect to the number of solvent molecules and recognizing that, at swelling equilibrium, the total chemical potential of the solvent in the gel equals the chemical potential of the solvent in the bulk,[35] we obtain eq B2.

$$\pi \cong \mu_{sol} - \mu_{os} = \mu_{mix} + \mu_{el} \tag{B2}$$

Thus, the osmotic swelling pressure is equal to the difference between the chemical potential of the solvent in the bulk solution, μ_{sol}, and the chemical potential of the solvent in the gel, μ_{os}. The μ_{mix} and μ_{el} terms in eq B2 are the polymer/solvent mixing contribution and the elastic contribution to the chemical potential of the gel, respectively.

Below we will present the expressions that were used to calculate π, μ_{el}, and μ_{mix} in eq B2 as a function of pH. Because each of these expressions may be written as a function of the swelling ratio $Q(=\phi^{-1})$, the solution of eq B2 at each pH provides the model prediction for the equilibrium swelling data shown in Figure 2.

Since the microgels behave as if they are in the low-salt limit (see below), to calculate the osmotic pressure, we apply the equation given by Shibayama et al. for the pressure due to the translational entropy of the counterions (eq B3).[35]

$$\pi = kT\frac{\phi}{A} \tag{B3}$$

In eq B3, A is the number of monomers between charged monomers, and ϕ is the volume fraction of polymer in the microgel.

To calculate the osmotic pressure as a function of pH in eq B3, we needed to calculate the value of A at each experimental pH. To determine A, a Donnan model that included ion binding was used.[2] According to the Donnan theory, the concentration of fixed charges on one side of a semipermeable membrane affects the distribution of all the diffusible ions between the two volumes separated by the membrane. For ionic microgels, which have negative acrylic acid groups that cannot move out of the gel, the solution within the microgel can be regarded as separated from the external solution by an equivalent semipermeable membrane. The "membrane" confines the fixed charges but permits the free passage to water and all small monovalent ions.

We have defined the concentrations of dissociated carboxyl groups as $[R^-]$, carboxyl groups bound with protons as [RH], carboxyl groups bound with sodium as [RNa], protons as $[H^+]$, hydroxyl ions as $[OH^-]$, sodium ions as $[Na^+]$, and chloride ions as $[Cl^-]$. The

subscripts m and s in the equations below refer to the microgel and external solution, respectively.

For a given pH and NaCl concentration in the bulk solution, the acid groups inside the microgel were assumed to have a concentration c and a degree of dissociation α ($= 1/A$), yielding a concentration of acid groups in undissociated form of $c\alpha$. The concentration of hydroxyl ions was related to the concentration of protons in each phase by the hydrolytic constant of water, K_w. The sum of the concentration of carboxyl groups that were bound with both hydrogen and sodium ions was equal to the total concentration of groups that were bound, $c(1 - \alpha)$. By applying the condition of electroneutrality, the concentration of Na^+ in both the microgel and the external solution was expressed as a function of the concentration of the other positive and negative ions in each solution.

Equation B4 gives an expression for the fraction of ionized groups in the microgel as a function of the binding constants of protons (K_a) and sodium (K_{Na}) as well as the concentrations of protons ($[H^+]$) and sodium ($[Na^+]$) in the microgel.

$$\alpha = \frac{K_a K_{Na}}{[H^+]_m K_{Na} + [Na^+]_m + K_a K_{Na}} \tag{B4}$$

Using the concentrations of the diffusible ions in the bulk solution, the appropriate Donnan equilibrium for the model is given by eq B5, where λ is the Donnan ratio.

$$\lambda = \frac{[H^+]_m}{[H^+]_s} = \frac{[Na^+]_m}{[Na^+]_s} = \frac{[OH^-]_m}{[OH^-]_s} = \frac{[Cl^-]_m}{[Cl^-]_s} \tag{B5}$$

By combining the first two ratios in eq B5, eq B6 is obtained.

$$\lambda = \frac{\dfrac{K_w}{[H^+]_m} + [Cl^-]_m + c\alpha}{\dfrac{K_w}{[H^+]_s} + [Cl^-]_m} \tag{B6}$$

By substituting $\lambda[H^+]_s$ for $[H^+]_m$, and $[Cl^-]_s/\lambda$ for $[Cl^-]_m$ from eq B5, eq B7 is obtained.

$$\lambda = \sqrt{1 + \frac{c\alpha}{\dfrac{K_w}{\lambda[H^+]_s} + \dfrac{[Cl^-]_s}{\lambda}}} \tag{B7}$$

Equation B7 provided an expression for λ as a function of α ($= 1/A$), the external ion concentrations (which were set experimentally), and the carboxyl group concentration inside the microgels (calculated from the experimental results). Substituting eq B4 into eq B7 resulted in a fourth-order equation in λ, with λ as the only unknown variable. The roots of this equation at each bulk solution pH and NaCl concentration were evaluated using Mathematica (Version 3.0, Wolfram Research, Inc.). Of the four roots, three were eliminated as possible solutions because they were negative. The one positive root, the only root that made physical sense for a Donnan ratio, was used in all subsequent calculations. From the value for λ that was obtained at each pH, the corresponding value of α ($= 1/A$) was obtained.

The inputs to the Donnan model were as follows. A bulk NaCl concentration of 0.03 M (set experimentally) was used. The carboxyl group concentration at each pH was calculated by dividing the total number of carboxyl groups (5.7 mequiv/g as measured by bulk titration) by the microgel volume at each pH (measured by micropipet manipulation). The apparent pK_a of 4.7 that was measured in the bulk titration was used to set the binding constant of protons. A value for K_{Na}, the binding constant of sodium to carboxyl groups, of 0.25 M based upon binding constants in the literature was used in the model.[2]

The chemical potential due to mixing, μ_{mix}, can be described by the Flory−Huggins equation (eq B8),[36] in which ϕ is defined as the polymer volume fraction in the gel and χ is the Flory interaction parameter.

$$\mu_{mix} = kT(\ln(1 - \phi) + \phi + \chi\phi^2) \tag{B8}$$

In the classical Flory theory, at constant temperature and for a fixed polymer composition, χ is treated as a constant.[45] However, in the case of anionic hydrogels that undergo a pH-induced condensation, the χ parameter cannot be treated as a constant. The hydrophilic/hydrophobic balance of the microgel matrix changes with pH when protons bind to the polymer backbone. As a result, a microgel changes from a polymer matrix for which water is a good solvent ($\chi < 0.5$) to one for which water is a poor solvent ($\chi > 0.5$). The result is that, at low pH, the microgel matrix collapses and squeezes out water.

An empirical equation describing the dependence of the χ parameter on the polymer volume fraction for both ionic and nonionic hydrogels has been determined to have the form[30,45−48]

$$\chi = \chi_o + b\phi \tag{B9}$$

where χ_o is the Flory parameter of the polymer at infinite dilution and b is the slope. The values for χ_o and b have been determined experimentally for several polymer/water slab gel systems by elastic moduli measurements (Table 2).

Unfortunately, there were no experimentally measured values for the concentration dependence of the Flory parameter of our microgels. Thus, we used best fit values within the range of those published for the comparable polymer systems shown in Table 2.[30,45−48] For χ_o and b the same values of 0.45 and 0.49 were used respectively in the case of all four FR microgels. Note that because this is an empirical equation, additional factors may be contained in it. Because the variation in cross-link density for the four microgels under investigation is relatively small (range of feed ratio = ±0.1 mole fraction units) following Freed et al., we thought it valid to use the same relationship to model each of the different cross-link density microgels.[49]

The chemical potential due to the polymer elasticity in eq B2 can be described by an expression that assumes non-Gaussian chain statistics. The use of a non-Gaussian expression is appropriate for the highly cross-linked microgels, which have polymer chains that contain fewer than 20 monomers between cross-links as based upon the monomer feed ratio.[13]

There have been several treatments of the swelling of a non-Gaussian polymer network.[13,50,51] In our analysis we use the expression derived by Kovac (eq B10) because it is mathematically simpler than the inverse Langevin approximation used previously and gives

quantitatively similar results.[50] The equation is

$$\mu_{el} = \frac{kT\rho V_1\phi}{M_{mer}N}\left(1 + \frac{2}{N}\phi^{-2/3} + \frac{1}{N^2}\phi^{2/3}\right)\left(1 - \frac{3}{N}\phi^{-2/3} + \frac{3}{N^2}\phi^{-4/3} + \frac{1}{N^3}\phi^{-2}\right)^{-1} \quad \text{(B10)}$$

where ρ is the density of the polymer, V_1 is the molar volume of the solvent, ϕ is the polymer volume fraction, M_{mer} is the mer average molecular weight, and N is the number of monomers between cross-links.

Substituting the expressions for the osmotic, mixing, and elastic contributions to the chemical potential, given by eqs B3, B8, and B10, respectively, into eq B2 results in eq B11.

$$\frac{\phi}{A} - \phi - \log(1-\phi) - \chi\phi^2 = \frac{\rho V_1\phi}{M_{mer}N}\left(1 + \frac{2}{N}\phi^{-2/3} + \frac{1}{N^2}\phi^{2/3}\right)\left(1 - \frac{3}{N}\phi^{-2/3} + \frac{3}{N^2}\phi^{-4/3} + \frac{1}{N^3}\phi^{-2}\right)^{-1} \quad \text{(B11)}$$

Equation B11 can be solved numerically for ϕ, and by doing so, we obtained a value for the swelling ratio Q ($= \phi^{-1}$) at each pH.

References and Notes

(1) Kawaguchi, H.; Fujimoto, K.; Saito, M.; Kawsaki, T.; Urakami, Y. *Polym. Int.* **1993**, *30*, 225−231.
(2) Eichenbaum, G.; Kiser, P.; Simon, S.; Needham, D. *Macromolecules* **1998**, *31*, 5084−5093.
(3) Ricka, J.; Tanaka, T. *Macromolecules* **1984**, *17*, 2916−2921.
(4) Peppas, N. In *Hydrogels in Medicine and Pharmacy*; Peppas, N., Ed.; CRC Press: Boca Raton, FL, 1986; Vol. 1, pp 27−56.
(5) Kim, S.; Bae, Y.; Okano, T. *Pharm. Res.* **1992**, *9*, 283−290.
(6) Molday, R. S.; Dreyer, W. J.; Rembaum, A.; Yen, S. P. *J. Cell Biol.* **1975**, *64*, 75−88.
(7) Rembaum, A.; Yen, S.; Cheong, E.; Wallace, S.; Molday, R.; Gordon, I.; Dreyer, W. *Macromolecules* **1976**, *9*, 328−336.
(8) Shiroya, T.; Tamura, N.; Yasui, M.; Fujimoto, K.; Kawaguchi, H. *Colloids Surf. B* **1995**, *4*, 267−74.
(9) Achiha, K.; Ojima, R.; Kasuya, Y.; Fujimoto, K.; Kawaguchi, H. *Polym. Adv. Technol.* **1995**, *6*, 534−40.
(10) Kawaguchi, H. *Front. Biomed. Biotechnol.* **1996**, *3*, 157−168.
(11) Kiser, P.; Wilson, G.; Needham, D. *Nature* **1998**, *394*, 459−462.
(12) Kiser, P.; Needham, D.; Wilson, G. *Proc. Am. Chem. Soc.: Div. Polym. Mater. Sci. Eng.* **1997**, *76*, 226.
(13) Peppas, N. *Hydrogels in Medicine and Pharmacy;* CRC Press: Boca Raton, FL, 1986; Vol. I.
(14) Peppas, N. A. *J. Biomed. Mater. Res.* **1985**, *19*, 397−411.
(15) Shibayama, M.; Fumiyoshi, I. *J. Chem. Phys.* **1997**, *107*, 5227−5235.
(16) Lee, Y.; Lee, S.; Jeong, D. *Polymer* (*Korea*) **1998**, *22*, 741−748.
(17) *Synthetic Hydrogels for Biomedical Applications*; Andrade, J., Ed.; American Chemical Society: Washington, DC, 1976; Vol. 31.
(18) Hoffman, A. S. In *NATO ASI Series*; Piskin, E. a. H. A. S., Ed.; Martinus Nijhoff Publishers: Dordrecht, The Netherlands, 1986; Vol. 106.
(19) Inoue, T.; Chen, G.; Nakamae, K.; Hoffman, A. *J. Controlled Release* **1997**, *49*, 167−176.
(20) Nakamae, K.; Nizuka, T.; Miyata, T.; Furukawa, M.; Nishino, T.; Kato, K.; Inoue, T.; Hoffman, A.; Kanzaki, Y. *J. Biomater. Sci., Polym. Ed.* **1997**, *9*, 43−53.
(21) Park, K. *Biodegradable Hydrogels for Drug Delivery*; Technomic Publishing Company, Inc.: Lancaster, PA, 1993.
(22) Antonsen, K.; Bohnert, J.; Nabeshima, Y.; Sheu, M.; Wu, X.; Hoffman, A. *Biomater., Artif. Cells, Immobilization Biotechnol.* **1993**, *21*, 1−22.
(23) Kawaguchi, H.; Kawahara, M.; Yaguchi, N.; Hoshino, F.; Ohtsuka, Y. *Polym. J.* **1988**, *20*, 903−9.
(24) Kashiwabara, M.; Fujimoto, K.; Kawaguchi, H. *Colloid Polym. Sci.* **1995**, *273*, 339−345.
(25) Sayle, R.; Milner-White, E. *Trends Biochem. Sci.* **1995**, *20*, 374.
(26) Loudon, G. *Organic Chemistry*, 2nd ed.; Benjamin/Cummings Publishing Company Inc.: Menlo Park, CA, 1988.
(27) Padmanabhan In *Analytical Profiles of Drug Substances*; Florey, K., Ed.; Academic Press: New York, 1983; Vol. 12, pp 105−134.
(28) Arcamone, F. *Doxorubicin Anticancer Antibiotics*; Academic Press: New York, 1981.
(29) Helfferich, F. *Ion Exchange*; McGraw-Hill Book Company: New York, 1962.
(30) Hasa, J. *J. Polym. Sci., Polym. Phys. Ed.* **1975**, *13*, 263−274.
(31) Gregor, H. *J. Am. Chem. Soc.* **1951**, *73*, 643−650.
(32) *Burger's Medicinal Chemistry*, 4th ed.; Wolff, M., Ed.; John Wiley & Sons: New York, 1981; Vol. 3.
(33) Meylan, W.; Howard, P. *J. Pharm. Sci.* **1995**, *84*, 83−92.
(34) Brannon-Peppas, L.; Peppas, N. *Chem. Eng. Sci.* **1991**, *46*, 715−722.
(35) Shibayama, M.; Tanaka, T. *Adv. Polym. Sci.* **1993**, *109*, 1−62.
(36) Flory, P. J. *Principles of Polymer Chemistry*; Cornell University Press: Ithaca, NY, 1953.
(37) Grignon, J.; Scallan, A. *J. Appl. Polym. Sci.* **1980**, *25*, 2829−2843.
(38) Firestone, B.; Siegal, R. *Biomater. Sci., Polym. Ed.* **1994**, *5*, 433−450.
(39) English, A.; Mafe, S.; Manzanares, J.; Yu, X.; Grosberg, A.; Tanaka, T. *J. Chem. Phys.* **1996**, *104*, 8713−8720.
(40) Tanaka, T.; Fillmore, D.; Sun, S.; Nishio, I.; Swislow, G.; Shah, A. *Phys. Rev. Lett.* **1980**, *45*, 1636−1639.
(41) Rubinstein, M.; Colby, R.; Dobrynin, A.; Joanny, J. *Macromolecules* **1996**, *29*, 398−406.
(42) Schossler, F.; Ilmain, F.; Candau, S. **1991**.
(43) Nanavati, C.; Fernandez, J. *Science* **1993**, *259*, 963−965.
(44) Tanaka, T.; Filmore, D. J. *J. Chem. Phys.* **1979**, *59*, 5151−5159.
(45) Kopecek, J.; Bazilova, H. *Eur. Polym. J.* **1974**, *10*, 465−470.
(46) Mikos, A.; Peppas, N. *Biomaterials* **1987**, *9*, 419−423.
(47) McKenna, G.; Korkay, F. *Polymer* **1994**, *35*, 5737−5742.
(48) McKenna, G.; Flynn, K.; Chen, Y. *Polym. Commun.* **1988**, *29*, 272−275.
(49) Freed, K.; Pesci, S. *Macromolecules* **1989**, *22*, 4048−4050.
(50) Kovac, J. *Macromolecules* **1977**, *11*, 362−365.
(51) Galli, A.; Brumage, W. *J. Chem. Phys.* **1983**, *79*, 2411−2418.
(52) Smith, R.; Martell, A. *NIST Critically Selected Stability Constants of Metal Complexes Database Version 3.0*; NIST: Texas, 1997.
(53) Bohdanecky, M.; Bazilova, H.; Kopecek, J. *Eur. Polym. J.* **1974**, *10*, 405−410.

MA981945S